DEFENSE TECHNICAL INFORMATION CENTER

Information for the Defense Community

DTIC® has determined on 10/7/2010 that this Technical Document has the Distribution Statement checked below. The current distribution for this document can be found in the DTIC® Technical Report Database.

☑ **DISTRIBUTION STATEMENT A.** Approved for public release; distribution is unlimited.

☐ **© COPYRIGHTED**; U.S. Government or Federal Rights License. All other rights and uses except those permitted by copyright law are reserved by the copyright owner.

☐ **DISTRIBUTION STATEMENT B.** Distribution authorized to U.S. Government agencies only (fill in reason) (date of determination). Other requests for this document shall be referred to (insert controlling DoD office)

☐ **DISTRIBUTION STATEMENT C.** Distribution authorized to U.S. Government Agencies and their contractors (fill in reason) (date of determination). Other requests for this document shall be referred to (insert controlling DoD office)

☐ **DISTRIBUTION STATEMENT D.** Distribution authorized to the Department of Defense and U.S. DoD contractors only (fill in reason) (date of determination). Other requests shall be referred to (insert controlling DoD office).

☐ **DISTRIBUTION STATEMENT E.** Distribution authorized to DoD Components only (fill in reason) (date of determination). Other requests shall be referred to (insert controlling DoD office).

☐ **DISTRIBUTION STATEMENT F.** Further dissemination only as directed by (inserting controlling DoD office) (date of determination) or higher DoD authority.

Distribution Statement F is also used when a document does not contain a distribution statement and no distribution statement can be determined.

☐ **DISTRIBUTION STATEMENT X.** Distribution authorized to U.S. Government Agencies and private individuals or enterprises eligible to obtain export-controlled technical data in accordance with DoDD 5230.25; (date of determination). DoD Controlling Office is (insert controlling DoD office).

Lasers in Surgery and Medicine 37:373–381 (2005)

Porcine Skin ED_{50} Damage Thresholds for 2,000 nm Laser Irradiation

Bo Chen, MS,[1]* Daniel C. O'Dell, BS,[1] Sharon L. Thomsen, MD,[1] Benjamin A. Rockwell, PhD,[2] and Ashley J. Welch, PhD[1]

[1]*Biomedical Engineering Laser Laboratory, The University of Texas at Austin, Austin, Texas*

[2]*Air Force AFRL/HEDO, Brooks City-Base, Texas*

Background and Objectives: To gain refinement in safe-exposure limits, indicated by the maximum permissible exposure (MPE) limits, the minimum visible lesion thresholds for three spot sizes (5–15 mm) and four exposure durations (0.25–2.5 seconds) were determined for the skin at 2,000 nm continuous wave laser irradiation.

Study Design/Materials and Methods: A series of experiments were conducted in vivo on female Yucatan mini-pigs to determine the ED_{50} damage thresholds for 2,000 nm continuous wave laser irradiation. The study employed Gaussian laser beam exposures with spot diameters ($1/e^2$) of 4.83, 9.65, and 14.65 mm and exposure durations of 0.25, 0.5, 1.0, and 2.5 seconds as a function of laser power. The effect of each irradiation was evaluated within 1 minute after irradiation and the final determination was made at 48 hours post-exposure. Probit analysis was conducted to estimate the dose for 50% probability of laser-induced damage (ED_{50}), defined as persistent redness at the site of irradiation for the mini-pig skin after 48 hours.

Results: The MPE spot size and exposure duration trends for 2,000 nm laser exposure is consistent for exposure diameters less than 3.5 mm. However, for larger exposure diameters of 4.83, 9.65, and 14.65 mm and exposure duration longer than 0.25 second, the current MPEs are bigger than one tenth of our damage thresholds. For Gaussian laser profile, which is common for many laser output irradiance distributions, lower energy is required to generate a lesion on skin for smaller spot sizes and shorter exposure duration. On the other hand, for spot sizes greater than 4.83 mm and exposure duration over 0.25 second, the average radiant exposure at threshold is inversely proportional to spot size. The irradiance-time and temperature-time power law at the threshold were investigated as well and showed that the irradiance-time power law was a close approximation to estimate laser irradiance at ED_{50} damage threshold.

Conclusions: The thresholds study shows that consideration for lowering the MPE standards should be explored as the laser beam diameter becomes larger than 3.5 mm. Based on the limited experimental data, the duration and size dependences of the ED_{50} damage thresholds could be described by an empirical equation: Irradiance at the threshold = (5.669 − 1.81 × spot diameter) × exposure duration$^{-0.794}$. Lasers Surg. Med. 37:373–381, 2005.

Key words: Gaussian laser irradiation; laser injury; laser safety; maximum permissible exposure (MPE); skin damage; visible lesion; Yucatan mini-pig

INTRODUCTION

Laser systems operating in the wavelength around 2,000 nm are in widespread use in military, medical, and industrial applications. Being relatively new to the medical fields, the Q switch and long pulse Ho:YAG lasers ($\lambda = 2.1$ μm) are principally used to precisely ablate bone and cartilage, with many applications in orthopedics for arthroscopy [1–3], urology for lithotripsy (removal of kidney stones) [4–6], otolaryngology for endoscopic sinus surgery [7–9], and spine surgery for endoscopic disc removal [10]. With the recent development of continuous-wave systems at 2,000 nm, it may be necessary to evaluate the need to refine the existing laser safety limiting exposure limits for these systems.

Maximum permissible exposure (MPE) is the level of radiation to which a person may be exposed without hazardous effect or adverse biological changes in the eyes and skin [11]. The MPEs for various wavelengths and pulse widths are defined by the American National Standards Institute (ANSI). This determination is done by the experts on the bioeffects subcommittee upon evaluation of minimum visible lesion threshold data, modeling, and understanding of the mechanisms for damage. The ANSI Z136.1-2000, American National Standard for Safe Use of Lasers [11] for skin at wavelengths between 1.8 and 2.6 μm and laser exposures from 1.0 millisecond to 10.0 second (see Table 1) is based on very little experimental data [12,13]. In this wavelength regime, the limited experiments have investigated cornea epithelial damage thresholds for exposure duration less than 0.25 second and laser spot size smaller than 1.8 mm.

Contract grant sponsor: Northrop Grumman Information Technology; Contract grant sponsor: The Albert and Clemmie Caster Foundation.

*Correspondence to: Bo Chen, MS, Biomedical Engineering Laser Laboratory, The University of Texas at Austin, Austin, Texas 78712. E-mail: chenbo@mail.utexas.edu

Accepted 18 August 2005
Published online in Wiley InterScience (www.interscience.wiley.com).
DOI 10.1002/lsm.20243

TABLE 1. Maximum Permissible Exposure (MPE) for Skin Exposure to a Laser Beam (From ANSI Z136.1-2000)[11]

Wavelength (μm)	Exposure duration, t (seconds)	MPE (J cm^{-2})	Limit aperture diameter (mm)
1,800–2,600	10^{-3}–10	$0.56\ t^{0.25}$	3.5

t is the laser exposure duration.

Studies on laser safety evaluate the MPE of the eye and the skin to laser irradiations. It is typically a factor of 10 below the ED_{50} damage threshold [14]. Exposure to levels at the published MPE values for the eye and skin may be "uncomfortable" [11]. Thus, it is good practice to maintain exposure levels sufficiently below the MPE to avoid discomfort [11]. In an effort to provide additional data for 2,000 nm laser safety standards, a series of experiments and tests were conducted on Yucatan mini-pigs to determine various parameters that inflict threshold damage on skin at 2,000 nm for large spot sizes (5–15 mm). Thresholds were determined in terms of the minimum visible lesion for exposure durations from 0.25 to 2.5 seconds.

The formation of thermally induced lesions in skin is a temperature-time rate process that is associated with the thermal denaturation of proteins [15]. The process begins with the local absorption of laser light in skin that is converted to heat. The localized heat source S [W/cm^3] at position $r(x,y,z)$ and time t is a function of the local wavelength dependent absorption coefficient μ_a[1/cm] of the laser light

$$S(r,t) = \mu_a(r)\phi(r,t) \quad (1)$$

Where $\phi(r,t)$ [W/cm^2] is the fluence rate at position $r(x,y,z)$ and time t. The primary absorbers, chromophores, for visible light and near IR radiation in skin are blood and melanin in the pigment epithelium. At 2,000 nm, water becomes the primary chromophore. Temperature $T(r,t)$ resulting from the absorbed laser light is governed by heat generation, storage, diffusion, and perhaps blood perfusion for long laser exposures. The actual pattern of light absorption is governed by light scattering at visible and near IR wavelengths. However, at wavelength above 1.4 μm where scattering is insignificant, light propagation can be described by Beer's law. When $\mu_a(r) = \mu_a$:

$$S(r,t) = \mu_a(1 - r_s)E(x,y,t)e^{-\mu_a z} \quad (2)$$

Where $E(x,y,t)$ [W/cm^2] is the irradiance and r_s is the specular reflectance from the skin surface [16].

The animal model that best represents black human skin is the Yucatan mini-pig. It is anatomically more similar to all human skin than the commonly used Yorkshire model [17]. The skin of the Yucatan mini-pig has less hair and increased density of melanin granules relative to the Yorkshire pig. The Yucatan mini-pig has dark skin color and, statistically, the flank skin thickness is approximately close to that of human face, arm, and neck skin, which have high probability of accidental exposure. By using this model, the properties of the human skin can be more closely approximated to gain a better understanding of human laser-tissue interaction for the wavelength of interest.

MATERIAL AND METHODS

Animal Preparation

The animal use protocol was approved by the Institutional Animal Care and Use Committee at the University of Texas at Austin. Six female Yucatan mini-pigs, weighing between 24.3 and 34.8 kg, were used in this study. Before beginning each of the experiments, the mini-pig was anesthetized initially with IM telazol-ketamine-xylazine (TKX) and intubated. Isoflurane (1%–3%) was administered for anesthesia maintenance throughout the procedure by a certified registered laboratory animal technologist. Heart rate, SpO_2, and respiration were monitored throughout the experiment. In addition, Carprofen (Rimadyl, Pfiser Limited, Kent, UK) was given at the end of the procedure to alleviate possible post-surgical pain. After the mini-pig was anesthetized, its hair was removed using Nair® depilatory. Nair® was removed 5 minutes after application and the mini-pig skin was bathed with Betadine and then water. The mini-pig was marked with a metallic-silver permanent marker to make grids for identification and location of the numerous irradiation sites. The dimensions of the grids depended upon the laser spot size.

Experimental Setup

A rack mountable fiber optic CW laser (IPG Photonics Corporation, Oxford, MA) with a maximum 20 W output at a wavelength 2,000 nm was used to create an array of irradiations. The output power was adjusted by changing the current on the front panel display. A power meter EPM2000 (Molectron Detector, Inc., Portland, OR) with air-cooled power meter probes PM30 or PM150 (Molectron Detector) was used to measure the output power corresponding to each current setting. Telescopes were employed to generate a collimated laser beam with desired spot diameters. A pulse generator (model DG535, Stanford Research Systems Inc., Sunnyvale, CA) was used to trigger laser output and control the exposure durations. The pulse generator also triggered a function generator (HP 33120A, Hewlett Packard Company, Palo Alto, CA), which controlled the imaging rate of an IR array detector thermal camera (Phoenix™ DAS camera system, Indigo, CA). The IR camera began capturing infrared images 0.1 second before the laser irradiation on the mini-pig skin, and continued recording for 4–9 seconds after the laser was turned off. The IR camera imaging rate was set at 100 frames per second.

The measurement system was arranged as depicted in Figure 1. Temperature calibration for the IR camera was done by using a blackbody heat source after laser irradiations on pig skin. The telescope and IR mirror were both mounted on the IR camera to ensure all burn sites were located at a fixed distance from the laser for the same spot size.

Three different laser spot sizes were produced by various telescopes. The laser beam profiles were measured using the knife-edge method [18] before conducting the mini-pig experiment, and were confirmed by temperature distribution taken by IR camera prior to heat conduction. Both the knife-edge method and the measured temperature distribution indicated that the laser beam profiles were nominally Gaussian with $1/e^2$ diameters of 4.83, 9.65, and 14.65 mm for the three telescope settings. The experimental uncertainty for spot diameter measurement by knife-edge method is 0.01 mm. An example of the measured skin surface temperature distribution after 30 milliseconds laser irradiation is illustrated in Figure 2 for a laser power of 3.23 W and spot diameter of 4.83 mm. The heat conduction in skin within 30 milliseconds is quite small and can be neglected. The temperature rise on the surface is linearly proportional to the irradiance and therefore can be used to represent the incident laser beam irradiance distribution.

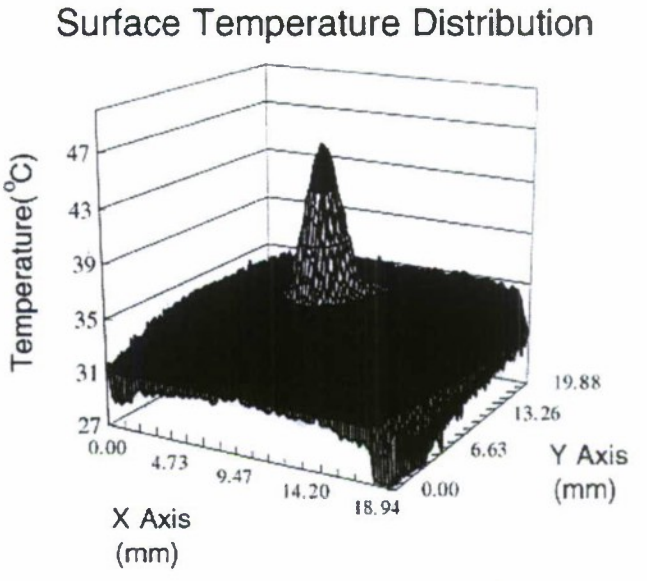

Fig. 2. Skin surface temperature distribution after 30 milliseconds laser irradiation. Laser power: 3.23 W, beam diameter: 4.83 mm.

Experimental Procedures

Radiant exposures were made at specified exposure durations of 0.25, 0.5, 1, and 2.5 seconds for spot diameters of 4.83, 9.65, and 14.65 mm. The number of irradiations for each of the 12 spot size-exposure conditions was 19–37 with an average of 27 per condition. The variation in laser power provided sufficient data points for probit analysis of damage/no damage response as a function of power. Forty-eight hours after laser irradiation, the size and type of lesions were observed and photographed by a digital camera (C-3040, Olympus Optical Co., Ltd., Japan) in order to find the ED_{50} damage threshold for the spot size-exposure conditions.

ED_{50} Damage Threshold Determination

To determine different degrees of damage and to choose a reliable and reproducible threshold of minimal visual laser-induced damage, a pilot study was conducted on a Yucatan mini-pig to generate damages from no visible lesion to tissue ablation and charring. Based on the 48-hours post-exposure reading, we defined the threshold thermal damage as grossly apparent persistent redness of the skin at the irradiation site at 48 hours. This kind of lesion was characterized as second-degree burn. More severe damage included epidermal roughening, blistering, and whitening coagulation of the underlying dermis. Based on visible skin damage/no damage (i.e., persistent redness), probit analysis was used to determine the ED_{50} damage threshold. Probit analysis [19,20] provided a statistically-estimated dose for 50% probability of minimal visual laser-induced damage (ED_{50}) for the mini-pig skin. Data points (damage/no damage for each condition) were entered into the probit statistical analysis package (Lund, B., Probit Fit Dose-Response Data Analysis Program, Version 1.02, U.S. Army Medical Research and Material Command, Hazards Research Branch) and the ED_{50} was calculated along with fiducial limits at the 95% confidence level.

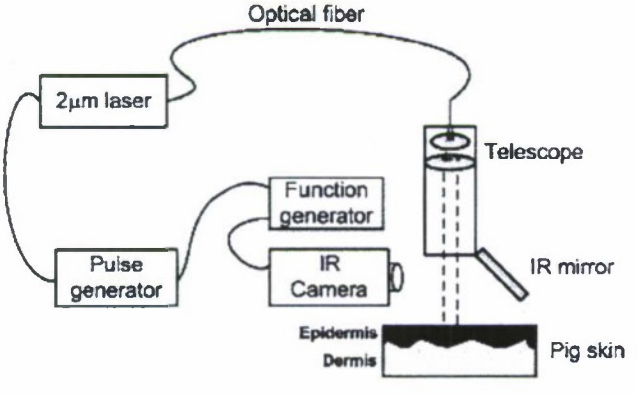

Fig. 1. Laser irradiation system with an IR camera.

In order to truly evaluate laser damage thresholds, average irradiance [W/cm^2] or radiant exposure [J/cm^2] reported in this paper was calculated as the applied laser power or energy divided by the $1/e^2$ spot area rather than $1/e$ spot area which is used in the laser safety classification. In fact, the peak irradiance or radiant exposure for our near Gaussian profile was twice the average value. Peak values were not reported.

RESULTS

ED_{50} Damage Threshold

Lesions around damage threshold initially appeared as red, flat spots on the skin at the site of irradiation. Most of

the lesions appeared instantly during laser irradiation on the skin. However, at some specific power level near the estimated threshold, redness developed on the skin several seconds after the laser irradiation took place and persisted in the 48-hours post-reading. Several red spots recorded immediately after irradiations were not observed at the 48-hours post-reading. However, the more common occurrence was that after 48 hours, near the threshold, thermal lesion formed flat red papules concomitantly with the shrinking of the epidermis at the center of irradiation sites. As laser power went higher than threshold, the size of red papules increased, and superficial ulcers occurred. Dark scabs were observed at 48 hours post-exposure when power was about 1.5–2 times the thresholds. In this case, coagulation and dehydration of the epidermis occurred. When the power was higher than four times of the thresholds, an audible pop accompanied with the abrupt temperature drop (the maximum skin temperature before drop reached around 160°C) was found. For this darkly pigmented skin, skin whitening, which was the usual symptom of third-degree burn, was not observed. Therefore, instead of whitening, persistent erythema (skin reddening) was the criterion on which the visible skin damage was based (Fig. 3).

The laser power for ED_{50} thresholds at 48-hours post-exposure readings are listed in Table 2. Standard deviation (σ) was derived from the probit fit curve by the definition:

$$\sigma = (ED_{84} - ED_{16})/2 \tag{3}$$

where ED_{84} represented the dose for 84% probability of laser-induced damage, and similarly for ED_{16}. An example of probit fit analysis for damage/no damage as a function of power is illustrated in Figure 4.

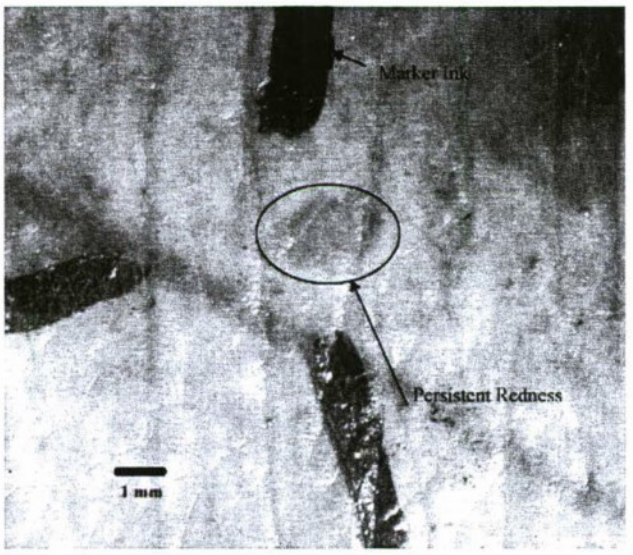

Fig. 3. A gross image of thermal lesion at the threshold. Laser condition: beam diameter 4.83 mm, exposure duration 0.25 second, laser power 2.84 W.

At some irradiation conditions, direct estimations were made without using probit analysis, because the data was quite consistent and there was insufficient scatter for the probit program. In other words, there was consistently damage or no damage above or below a specific exposure level (respectively). For instance, at 2.5 seconds exposure time and 9.65 mm diameter, there were constant damages at 1.57 W but no damage at the next lower possible power level of 1.25 W.

Even though the Yucatan mini-pig skin best represents human skin, the dark pigmentation of the skin hindered the visual determination of threshold damage, and therefore could have contributed to inflation in the ED_{50} value due to observational threshold differences. Other experimental uncertainties are mainly from the power measurements. The air-cooled power meter probes PM30 and PM150 have 3% uncertainties, and the power meter EPM2000 has 1% read-out error. However, these instrumental errors are relatively small to the uncertainty from visual damage determination.

Peak Temperature at ED_{50} Power

Peak temperature associated with ED_{50} power levels of Table 2 are presented in Table 3. Base-line temperatures were approximately 33°C. Peak temperature rise is defined as the maximum temperature rise at the irradiation center on the skin relative to the initial skin temperature at the start of radiation. Because of the Gaussian shape of the laser beam, peak temperature represents the temperature rise at the irradiation center.

Peak Temperature Rise with Respect to Power

Peak temperature rise as a function of laser power are presented in Figures 5a–c for spot diameters of 4.83, 9.65, and 14.65 mm, respectively. Linear fits were computed for peak temperature rises less than 70°C. (Note: scales are different between Fig. 5a–c)

DISCUSSION

It is usually assumed that infrared radiations at wavelengths above 1.4 μm are absorbed in a thin surface layer of the skin, thereby heating the tissue, and inducing an injury as the temperature increases. The conversion of radiant energy to thermal energy can produce damage, which can be predicted using the standard rate process model:

$$\Omega = \int_0^{\tau} A e^{-\left[\frac{E}{RT(t)}\right]} dt \tag{4}$$

where Ω is a dimensionless damage parameter, τ is the time, A is the pre-exponential frequency factor, E is an energy barrier molecules surmount in changing from native state to denatured, R is the gas constant, and T is the temperature [15]. The damage parameter Ω indicates the serious level of thermal injury on the skin, and, in this experiment, is set to be 1 for a second-degree burn indicated by a persistent red papule at 48 hours.

TABLE 2. The ED_{50} Power and Standard Deviation at Damage Thresholds* Followed by Lower and Upper 95% Confidence Limits

	Diameter (mm)		
Duration (seconds)	4.83	9.65	14.65
0.25	2.62 ± 0.28 W[a]	8.46 ± 1.04 W (8.46–8.46 W)	16.09 ± 0.43 W (15.18–16.65 W)
0.5	1.49 ± 0.48 W (0.08–1.91 W)	4.94 ± 0.27 W (4.94–4.94 W)	8.46 ± 0.80 W (8.08–9.48 W)
1.0	0.93 ± 0.29 W[a]	2.88 ± 0.35W[a]	5.02 ± 1.06 W (4.30–5.72 W)
2.5	0.41 ± 0.12 W (0.30–0.68 W)	1.41 ± 0.11 W[a]	2.46 ± 0.30 W (2.04–2.74 W)

*Thresholds of apparent persistent redness of the skin visible at 48 hours.
[a]Estimated without using probit fit.

The total exposure energy at the ED_{50} damage threshold (Table 4) is the product of the power and exposure time. Because the skin absorbs the irradiated energy linearly, the energy deposited into the skin is linearly proportional to the radiated energy. Table 4 shows that more energy is required to generate a visible lesion for longer laser exposure durations. This can be explained by the energy lost due to the heat conduction from hot to cool regions during the irradiation. Additionally, convection on the skin-air surface consumes some of the absorbed energy. Furthermore, blood under the heated skin surface will flow quicker than usual to cool down the higher temperature area. The longer the exposure time, the more energy is lost to the surrounding area. In other words, more energy is needed to raise skin temperature to the critical level that could generate lesions.

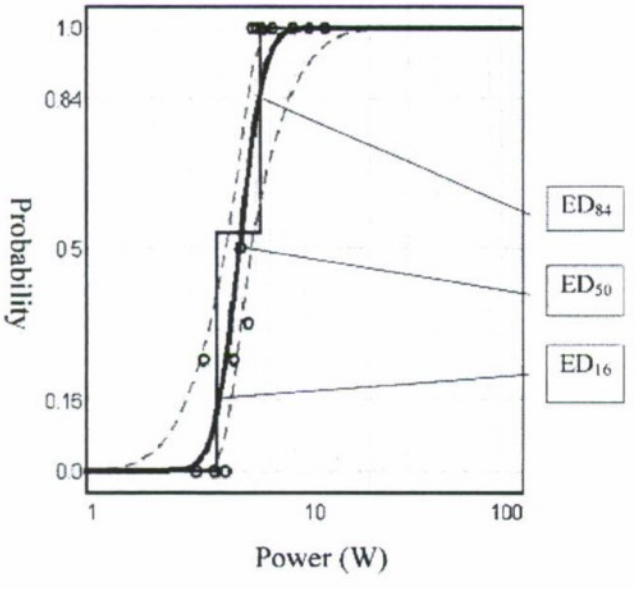

Fig. 4. Probit fit analysis to estimate ED_{50} damage threshold for 14.65 mm diameter laser spot and 1 second duration. The circles are the experimental data (the probabilities to find damage after irradiations) and the solid curve is the probit fit curve. Zero represents no damage and one represents damage. Some circles are not zero or one due to the variation of multiple measurements at the same power.

The ANSI standard of MPE for skin exposure to 2,000 nm laser and the experimental results of average energy fluence at ED_{50} damage threshold at various durations and beam sizes are compared in Table 5. Since the MPE level is established for a limiting aperture of 3.5 mm at this wavelength and these exposure durations, the larger spot sizes of our experiment provided additional data for the specification of safety standards for large spots. Table 5 displays the threshold energy divided by the laser spot area. The ED_{50} values for the four exposure times are slightly less than 10 times the corresponding MPEs but not inconsistent considering the inversely proportional size-dependence of ED_{50} values. Based on the experimental data, we can predict that the average energy fluence at ED_{50} damage thresholds for 3.5 mm diameter laser is about 10 times larger than MPE standard. Secondly, over the range of exposures, the MPE is larger than one tenth of the damage threshold. It means this MPE standard must be considered carefully and could be decreased as the beam diameter becomes larger than 3.5 mm. In conclusion, this experiment supports the need to reduce the MPE standard for NIR laser beams with 5–15 mm diameter.

One thing to be noted is that the laser beam diameter for non-uniform beam profiles are typically quoted at $1/e$ rather than $1/e^2$ to give more conservative radiant exposures to compare to published MPE values in the laser safety classification. The radiant exposure based on $1/e$ diameter is just twice as large as the $1/e^2$ diameter radiant exposure, and indicates the peak radiant exposure for a Gaussian shape laser beam. Although, $1/e$ diameter is a conservative

TABLE 3. The Peak Temperature Rise at ED_{50} Damage Thresholds

	Beam diameter (mm)		
Exposure duration (seconds)	4.83	9.65	14.65
0.25	42.5°C	32.3°C	33.9°C
0.5	39.6°C	30.3°C	29.0°C
1.0	38.5°C	27.9°C	26.8°C
2.5	31.4°C	25.4°C	22.9°C

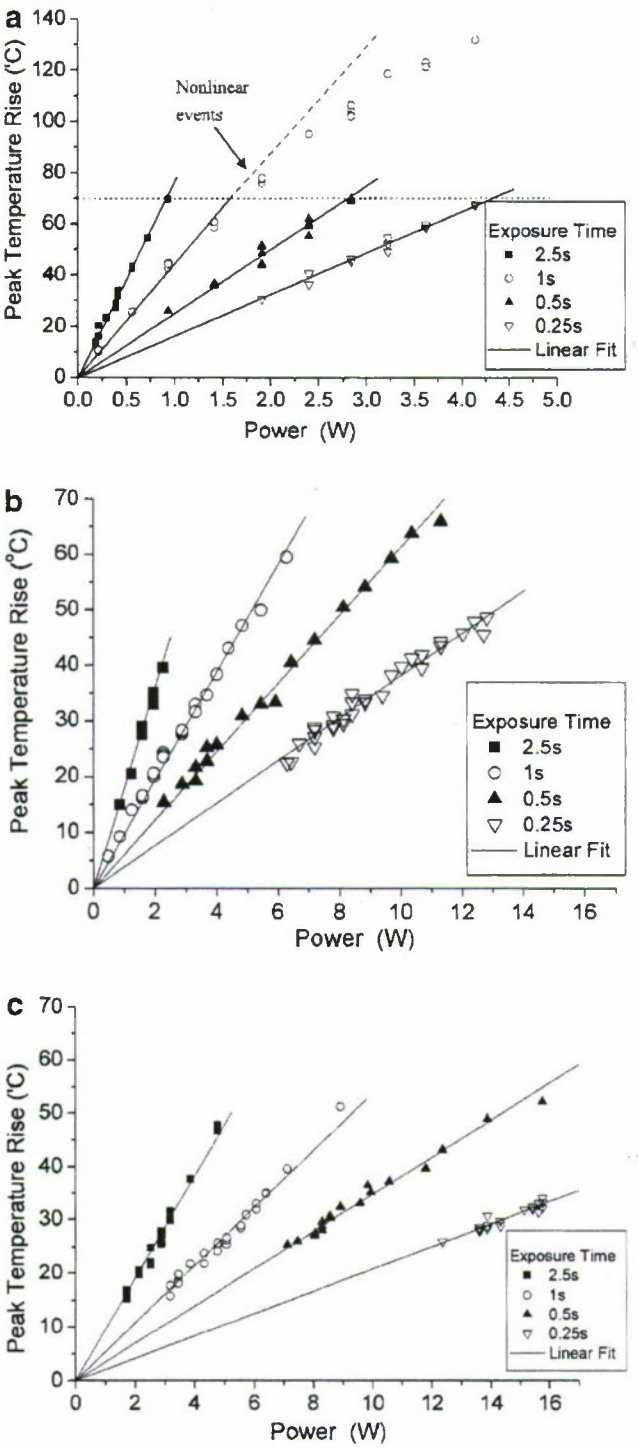

Fig. 5. **a**: Peak temperature rise versus power. Laser beam diameter 4.83 mm. Linear fits were computed for peak temperature rises less than 70°C. **b**: Peak temperature rise versus power. Laser beam diameter 9.65 mm. Note: scales are different between (a–c). **c**: Peak temperature rise versus power. Laser-beam diameter 14.65 mm.

estimation of the laser hazard classification, $1/e^2$ diameter must be used to truly evaluate laser damage thresholds, which require average irradiance.

Another feature evident from Table 5 is that the ED_{50} radiant exposure decreases with increasing spot size. This is due to the Gaussian shape of the laser beam and spot diameter dependent heat conduction that takes place during irradiation. Theoretically, if there is no heat transfer during laser irradiation, the temperature rise on the skin is linearly proportional to the local radiant exposure. However, the heat conduction cannot be ignored for durations longer than the characteristic diffusion time (actually longer than a tenth of the characteristic diffusion time), which is applicable to our experiments. The light $1/e$ penetration depth at 2,000 nm is approximately 200 μm and the associated characteristic diffusion time for a large spot diameter is about 300 milliseconds [21]. Heat conduction is described by

$$\frac{dT}{dt} = \frac{K}{\rho C_p}\nabla^2 T + \frac{Q}{\rho C_p} \tag{5}$$

where Q is the heat source term due to the laser irradiation in our experiments, T is the temperature, K is the thermal conductivity, ρ is the density, and C_p is the specific heat of tissue. The equation indicates that the temperature change with respect to time is directly proportional to $\nabla^2 T$. In this case, a laser spot with larger diameter have a flatter radiant exposure distribution so that smaller $\nabla^2 T$ is generated on the skin. Therefore, the temperature at the irradiation center increases quicker (less heat loss due to conduction) for larger beam sizes with the same radiant exposure. In other words, smaller radiant exposure is needed to generate ED_{50} lesions.

Although more energy is needed to generate a lesion on skin for longer laser exposure time, at the ED_{50} damage threshold, the peak temperature rise just after laser irradiation is in inverse proportion to exposure time (Table 3). Since thermal damage follows a rate process, a lower temperature rise is needed to generate a burn on skin for longer exposure time. Although the peak temperature provides an important aspect of the temperature trait on mini-pig skin, it does not necessarily represent the actual threshold temperature that is associated with the boundary between normal and significant thermal damaged tissue.

The average irradiance, exposure time, and surface peak temperature rise at ED_{50} damage threshold were investigated based on the power law relation postulated by Stoll and Greene in 1959 [22]. They investigated the relationship between pain and tissue damage due to white light irradiation using three human subjects. Based on the data they acquired a simple irradiance-time power law and a temperature-time power law:

$$E = At^{-B} \tag{6}$$

$$\Delta T = Ct^{-D} \tag{7}$$

were found, where A, B, C, D are positive constants, E is the irradiance at the threshold, ΔT is the temperature rise

TABLE 4. The Energy Irradiated on the Mini-Pig Skins at ED_{50} Damage Thresholds

Exposure duration (seconds)	Beam diameter (mm)		
	4.83	9.65	14.65
0.25	0.66 ± 0.07 J	2.12 ± 0.26 J	4.02 ± 0.11 J
0.5	0.75 ± 0.24 J	2.47 ± 0.14 J	4.23 ± 0.40 J
1.0	0.93 ± 0.29 J	2.88 ± 0.35 J	5.02 ± 1.06 J
2.5	1.03 ± 0.30 J	3.53 ± 0.28 J	6.15 ± 0.75 J

on skin at the threshold, and t is the exposure time. Figure 6a clearly shows that the irradiance-time power law can precisely describe our experimental results of irradiance at ED_{50} damage thresholds. Although coefficient A varies with respect to beam size, the power coefficient B is constant around 0.8, which is close to the Stoll's finding—$B = 0.74$ for thresholds of pain with burning. For a spot diameter around 15 mm, which is used in Stoll's experiment as well, the power law for laser-induced lesion is given by $E = (3.07\ \mathrm{W/cm^2})t^{-0.81}$. This is close to Stoll's finding when the skin tissue was irradiated by a white light projection lamp yielding an irradiance-time power law of $E = (2.82\ \mathrm{W/cm^2})t^{-0.74}$. Power-law coefficient A for various spot diameters are examined in Figure 7. A least square linear fit indicates there is a simple relationship between coefficient A and spot diameter d (cm)—$A = 5.669 - 1.81d$ (Fig. 7). In conclusion, the irradiation at the ED_{50} damage threshold could be predicted by this empirical equation $E = (5.669 - 1.81d)t^{-0.794}$ ($\mathrm{W/cm^2}$). Recalling the MPE standard and that the standard is a factor of 10 lower than threshold, the MPE radiant exposure is $H = 0.56t^{0.25}$ ($\mathrm{J/cm^2}$). For a spot diameter of 0.35 cm, the empirical power law gives a close estimation $H = 0.50t^{0.206}$ ($\mathrm{J/cm^2}$) (define the MPE radiant exposure as one tenth of the radiant exposure at the ED_{50} damage threshold). For $d = 1.465$ cm, the MPE radiant exposure from our estimation should be $0.302t^{0.206}$ ($\mathrm{J/cm^2}$). Although the empirical equation $E = (5.669 - 1.81d)t^{-0.794}$ ($\mathrm{W/cm^2}$) fits our threshold results quite well, it is obviously not suitable for much smaller or larger spot sizes. For spot diameters much larger than 15 mm, the irradiance at threshold should be independent of the spot size. On the other hand, for smaller spot diameters much less than 5 mm, the threshold irradiance will increase faster than this linear prediction [23,24]. For instance, McCally et al. [13] measured the cornea epithelial damage thresholds for 0.235 seconds exposure and 1.33 mm $1/e^2$ spot diameter at wavelength 2.02 μm. The measured threshold radiant exposure was 8.46 $\mathrm{J/cm^2}$, which is higher than the predicted value 4.03 $\mathrm{J/cm^2}$ from our linear empirical equation.

It is difficult to compare our results to data at other wavelengths and spot sizes since ED_{50} thresholds are functions of optical properties and spot sizes. Even when scattering can be neglected, differences in the absorption coefficient affect threshold. For example, the classical data of human skin laser damage thresholds [25] support a threshold for CO_2 irradiation for 1.05 cm diameter spot and 1 second exposure duration of 2.8 $\mathrm{J/cm^2}$ whereas our results report a value of 3.9 $\mathrm{J/cm^2}$ at 2.0 μm. The difference is due to penetration depths of the radiation for the two wavelengths. Radiation will penetrate deeper into skin at wavelength 2.0 μm rather than 10.6 μm; that is, more energy is needed for 2.0 μm radiation to increase skin temperature to the critical level that generates thermal damage.

Although irradiance and exposure time nearly fit the power law relation, peak temperature and exposure time have a much more complicated relationship. Figure 6b shows the linear fit line of the logarithmic exposure time and peak temperature rise. Neither coefficient C nor the exponential coefficient D remains constant for the different beam sizes. The main reason for these differences is that the laser beam used in this experiment was a Gaussian profile whereas uniform radiation on skin is reported in Stoll's experiment. Due to the non-uniform laser beam profile (i.e., Gaussian profile) on skin, the temperature changes with position, and the peak temperature does not represent the

TABLE 5. The Average Radiant Exposure [$\mathrm{J/cm^2}$] at ED_{50} Damage Thresholds

Exposure duration (seconds)	Beam diameter (mm)			
	4.83	9.65	14.65	3.5 (MPE from ANSI)
0.25	3.57 ± 0.38 $\mathrm{J/cm^2}$	2.89 ± 0.36 $\mathrm{J/cm^2}$	2.39 ± 0.06 $\mathrm{J/cm^2}$	0.396 $\mathrm{J/cm^2}$
0.5	4.07 ± 1.31 $\mathrm{J/cm^2}$	3.38 ± 0.18 $\mathrm{J/cm^2}$	2.51 ± 0.24 $\mathrm{J/cm^2}$	0.471 $\mathrm{J/cm^2}$
1.0	5.08 ± 1.58 $\mathrm{J/cm^2}$	3.94 ± 0.48 $\mathrm{J/cm^2}$	2.98 ± 0.63 $\mathrm{J/cm^2}$	0.560 $\mathrm{J/cm^2}$
2.5	5.59 ± 1.64 $\mathrm{J/cm^2}$	4.82 ± 0.38 $\mathrm{J/cm^2}$	3.65 ± 0.44 $\mathrm{J/cm^2}$	0.704 $\mathrm{J/cm^2}$

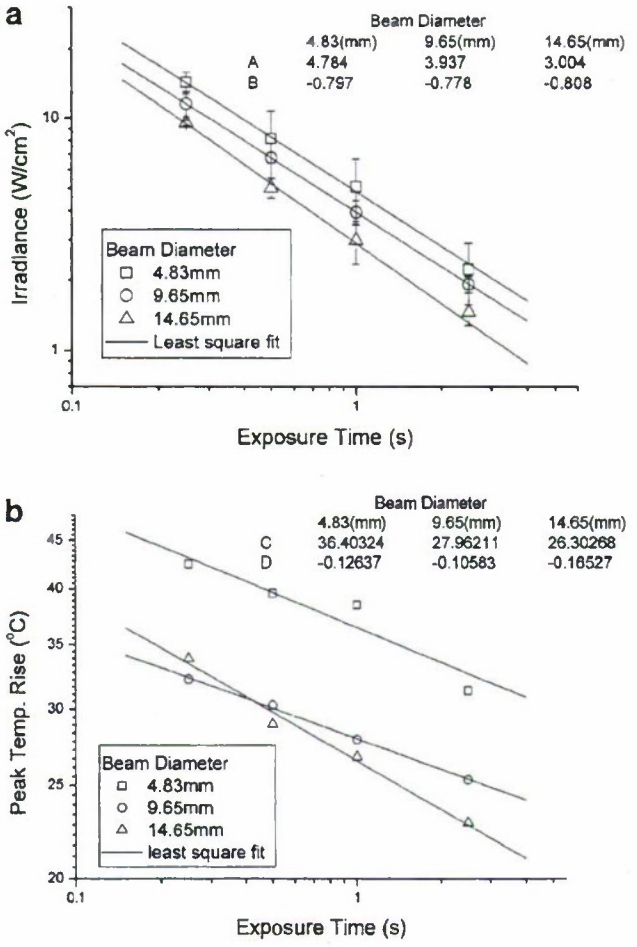

Fig. 6. **a**: The least square fit line of exposure time and irradiance, $E_T = At^B$. **b**: The least squared fit line of exposure time and peak temperature rise, $\Delta T = Ct^d$.

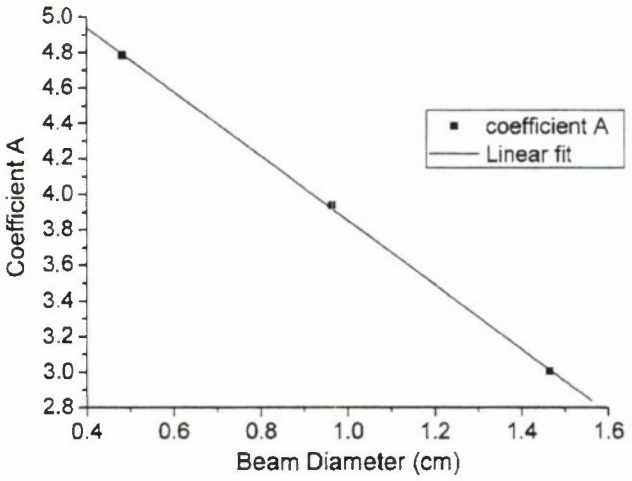

Fig. 7. Coefficient A for various diameters (d(cm)). Linear fit shows $A = 5.669 - 1.81d$.

actual threshold temperature that is associated with the boundary between normal and significant thermal damaged tissue.

Linear fits of the peak temperature rise with respect to power (Fig. 5a–c) show that the peak temperature response is linearly proportional to the laser power when peak temperature rise is below 70°C. This indicates that the optical and thermal properties of the skin tissue, such as absorption, scattering, and thermal conduction, do not significantly vary during heating. Furthermore, even though the redness caused by stepped-up blood flow has been discovered during irradiation, the conduction of heat energy away from the skin surface by way of the blood perfusion is insignificant compared to thermal conduction in the tissue. In other words, the increased blood flow does not significantly cool the skin surface during the laser irradiations in these experiments. The linear heat conduction equation predicts that temperature rise is proportional to absorbed energy. That is, the temperature response at $T(x,y,z,t)$ scales with power. The surface temperature of the mini-pig skin is about 33°C, so the turning point of this linear trend is around 100°C, the boiling point of water. The vaporization of water from the tissue surface is probably the reason for the discontinuation of linearity. As water diffuses from tissue, local thermal properties of conductivity, heat capacity, and density are altered [16]. Moreover, the optical properties of the skin undoubtedly changes around 100°C, and contributes to the discontinuation of linearity as well. Visual observation notes that irradiated mini-pig skin which is heated to 100°C or higher temperature becomes much darker and brittle on the surface. Even above 100°C, tissue may not be ablated but in a super heated state owing to the strength of the epidermis preventing the escape of water vapor.

CONCLUSION

We have measured the minimum visible lesion thresholds in Yucatan mini-pig skin for three different laser spot sizes at four various pulse durations. For a CW 2,000 nm wavelength laser, the irradiance exposure-time power law has been evaluated based on the experimental results of the average irradiance values at the thresholds. It shows that the average irradiance at the ED_{50} damage threshold has a simple power law relation to exposure time $E = (5.669 - 1.81d)t^{-0.794}$ (W/cm^2). This simple empirical equation reveals the duration and size dependences of the ED_{50} damage thresholds. For Gaussian shape laser irradiation, which is common in many laser medical applications, lower energy is needed to generate a lesion on skin for smaller spot sizes, and shorter exposure durations. On the other hand, the average radiant exposure at threshold is inversely proportional to spot size. These effects occur due to the Gaussian shape of the laser beam and the heat transfer during irradiation. The peak temperature rise at threshold and the corresponding exposure time may have a more complicated relationship that is not explained by simple power law relation.

We calculate the MPE from ANSI standards for 2,000 nm wavelength at the exposure duration used in the experiments and conclude that the MPE standard is reasonable for the original 3.5 mm spot diameter, but larger than necessary for 4.83, 9.65, and 14.65 mm spot sizes and exposure durations of 0.25 second and longer. For our criterion of damage, the MPEs are bigger than one tenth of ED_{50} damage thresholds; therefore the MPE standard should be considered carefully and could be decreased as the laser beam diameter becomes larger than 3.5 mm.

ACKNOWLEDGMENTS

Opinions, interpretations, conclusions, and recommendations are those of the authors and are not necessarily endorsed by the University of Texas, the United States Air Force or the Department of Defense.

The authors thank Dr. Darrell Tata, Dr. Robert J. Thomas, Dr. Sergey Telenkov, Victor Villavicencio, Dan Polhamus, and Jennifer Cassaday for their kind help.

REFERENCES

1. Trauner K, Nishioka N, Patel D. Pulsed holmium: Yttrium-aluminum-garnet (Ho:YAG) laser ablation of ®brocartilage and articular cartilage. Am J Sports Med 1990;18(3):316–320.
2. Trauner KB, Nishioka NS, Flotte T, Patel D. Acute and chronic response of articular cartilage to holmium:YAG laser irradiation. Clin Orthop 1995;310:52–57.
3. Gerber BE, Asshauer T, Delacretaz G, Jansen T, Oberthur T. Biophysical bases of the effects of holmium laser on articular cartilage and their impact on clinical application technics. Orthopade 1996;25(1):21–29.
4. Yiu MK, Liu PL, Yiu TF, Chan AYT. Clinical experience with holmium:YAG laser lithotripsy of ureteral calculi. Lasers Surg Med 1996;19:103–106.
5. Razvi HA, Denstedt JD, Chun SS, Sales JL. Intracorporeal lithotripsy with the holmium:YAG laser. J Urol 1996;156:9–12.
6. Das A, Erhard MJ, Bagley DH. Intrarenal use of the holmium laser. Lasers Surg Med 1996;19:103–106.
7. Oswal VH, Bingham BJG. A pilot study of the holmium YAG laser in nasal turbinate and tonsil surgery. J Clin Laser Med Surg 1992;10:211–216.
8. Shapshay SM, Rebeiz EE, Pankratov MM. Holmium: Yttrium aluminium garnet laser-assisted endoscopic sinus surgery: Clinical experience. Laryngoscope 1992;102:1177–1180.
9. Shapshay SM, Rebeiz EE, Bohigian RK. Holmium: Yttrium aluminium garnet laser-assisted endoscopic sinus surgery: Laboratory experience. Laryngoscope 1991;101:142–149.
10. Min K, Leu H, Zweifel K. Quantitative determination of ablation in weight of lumbar intervertebral discs with Holmium:YAG laser. Lasers Surg Med 1996;18:187–190.
11. American National Standards Institute. ANSI Z136.1-2000, American National Standard for safe use of lasers. Laser Institute of America, Orlando, FL, 2000.
12. Lund DJ, Beatrice ES, Stuck BE. Biological research in support of project MILES. Letterman Army Institute of Research Report—Institute Report No. 96, 1981.
13. McCally RL, Farrell RA, Bargeron CB. Cornea epithelial damage thresholds in rabbits exposed to Tm:YAG laser radiation at 2.02 microns. Lasers Surg Med 1992;12:598–603.
14. Sliney D, Wolbarsht M. Safety with lasers and other optical sources. New York: Plenum Press. 1980.
15. Henriques FF. Studies of thermal injury V. Arch Pathol 1947;43:489–502.
16. Takata AN. Laser-induced thermal damage of skin. USAF School of Aerospace Medicine, Brooks Air Force Base, TX. 1977.
17. Eggleston TA, Roach WP, Mitchell MA, Smith K, Oler D, Johnson TE. Comparison of two porcine (*Sus scrofa domestica*) skin models for in vivo near-infrared laser exposure. Comp Med 2000;50(4):391–397.
18. Siegman AE, Sasnett MW, Johnston JTF. Choice of clip levels for beam width measurements using knife-edge techniques. IEEE J Quantum Electron 1991;27:1098–1104.
19. Finney DJ. Probit Analysis, 3rd ed. New York: Cambridge University Press. 1971.
20. Cain CP, Noojin GD. A comparison of various probit methods for analyzing yes/no data on a log scale. Brooks AFB, TX: USAF Armstrong Laboratory; AL/OE-TR-1996-0102;1996.
21. Jacques SL. Role of tissue optics and pulse duration on tissue effects during high-power laser irradiation. App Optics 1993;32(13):2447–2454.
22. Stoll AM, Greene LC. Relationship between pain and tissue damage due to thermal irradiation. J App Physiol 1959;14(3):372–382.
23. Tan OT, Motemedi M, Welch AJ, Kurban AK. Spotsize effects on guinea pig skin following pulsed irradiation. J Invest Dermatol 1988;90(6):877–881.
24. Keijzer M, Pickering JW, van Gemert MJC. Laser beam diameter for port wine stain treatment. Lasers Surg Med 1991;11:601–605.
25. Rockwell RJ, Jr., Goldman L. Research on human skin laser damage threshold. Final report, Conract F41609-72-C-0007. USAF School of Aerospace medicine, Brooks Air Force Base, TX. 1974.